

Estimating spatially varying health effects of wildland fire smoke using mobile health data

Lili Wu^{*1}, Chenyin Gao^{*1}, Shu Yang^{†1}, Brian J. Reich¹, and Ana G. Rappold²

¹Department of Statistics, North Carolina State University, Raleigh, U.S.A.

²Environmental Protection Agency, Research Triangle Park, Durham, U.S.A.

July 9, 2024

Abstract

Wildland fire smoke exposures are an increasing threat to public health, and thus there is a growing need for studying the effects of protective behaviors on reducing health outcomes. Emerging smartphone applications provide unprecedented opportunities to deliver health risk communication messages to a large number of individuals when and where they experience the exposure and subsequently study the effectiveness, but also pose novel methodological challenges. Smoke Sense, a citizen science project, provides an interactive smartphone app platform for participants to engage with information about air quality and ways to protect their health and record their own health symptoms and actions taken to reduce smoke exposure. We propose a new, doubly robust estimator of the structural nested mean model parameter that accounts for spatially- and time-varying effects via a local estimating equation approach with geographical kernel weighting. Moreover, our analytical framework is flexible enough to handle informative missingness by inverse probability weighting of estimating functions. We evaluate the new method using extensive simulation studies and apply it to Smoke Sense data reported by the citizen scientists to increase the knowledge base about the relationship between health preventive measures and improved health outcomes. Our results estimate how the protective behaviors' effects vary over space and time and find that protective behaviors have more significant effects on reducing health symptoms in the Southwest than the Northwest region of the USA.

Keywords: Balancing criterion; Causal inference; Non-response instrument; Treatment heterogeneity; Smoke Sense

*Joint first authors

†Corresponding Author: Department of Statistics, North Carolina State University, 2311 Stinson Dr. Raleigh, NC 27695, Raleigh, U.S.A.

E-mail: syang24@ncsu.edu

1 Introduction

Wildland fire smoke is an emerging health issue as one of the largest sources of unhealthy air quality, attributing an estimated 340,000 excess deaths each year globally (Johnston et al., 2012). Although there are a number of exposure-reducing actions recommended, there is a lack of evidence of the long-term reduction in the number of adverse health outcomes by taking health-protective behaviors (treatments). The Smoke Sense citizen science initiative (Rappold et al., 2019), introduced by the researchers at the Environment Protection Agency, aims to engage citizen scientists and develop a personal connection between changes in environmental conditions and changes in personal health to promote health-protective behavior during wildland fire smoke exposure. The overarching objective of the Smoke Sense project is to develop and maintain an interactive platform for building knowledge about wildfire smoke, health, and protective actions to improve public health outcomes. The use of smartphone application (app) is designed as a risk reduction intervention based on the theory of planned behavior and health belief model. Through Smoke Sense, participants can report their perceptions of risk, adoptions of protective health behaviors and health symptoms. Therefore, Smoke Sense is uniquely placed to address this knowledge gap.

App-based platforms provide unprecedented opportunities to reach users and learn about the personal motivations to engage with the information delivered through the apps. However, the data also present analytical and methodological challenges as summarized below. (i) Adoption of health-protective behaviors (treatments) were left to the participants and may depend on the participant’s characteristics and perceptions of benefits and barriers of these actions. Self-selection can potentially result in confounding by indication (Pearl, 2009). Thus, statistical methods must adequately adjust for participant characteristics that confound the relationship between their behaviors and the outcome. This challenge is more pronounced in longitudinal Smoke Sense data because of the time-varying treatments and confounding. (ii) Although participants can be viewed as independent samples, the causal effect of treatment may vary over the study’s large and socially- and environmentally-diverse domain that is not explained by the observed covariates, and existing causal methods typically assume the structural treatment effect model accounting for the observed covariates is homogeneous. (iii) Participants were more likely to self-report when they experienced smoke or had health symptoms, leading to informative non-responses (Rubin, 1976); i.e., the missingness mechanism due to non-responses depends on the missing values themselves even adjusting for all observed variables. Failure to appropriately account for informative missingness may also lead to bias. These opportunities and challenges are identified for the Smoke Sense citizen science platform; however, a causal inference framework to study the relationship between interventions and health outcomes from mobile application data would have wider application in health and behavior research.

Confounding by indication poses a unique challenge to drawing valid causal inference of treatment effects from observational studies. For example, sicker patients are more likely to take the active treatment, whereas healthier patients are more likely to take the control treatment. Consequently, it is not meaningful to compare the outcome from the treatment group and the control group directly. Moreover, in longitudinal observational studies, confounding by indication is likely to be time-dependent (Robins and Hernán, 2009), in the sense that time-varying prognostic factors of the outcome affect the treatment assignment at each time, and thereby distort the association between treatment and outcome over time. In these cases, the traditional regression methods are biased even after adjusting for the time-varying confounders (Robins et al., 1992).

Parametric g-computation (Robins, 1986), Marginal Structural Models (Robins 2000), and Structural Nested Models (Robins et al., 1992) are three major approaches to overcoming the challenges with time-varying confounding in longitudinal observational studies. However, the

existing causal models typically assume the spatial homogeneity of the structural treatment effect models accounting for the observed covariates; i.e., the treatment effect is a constant across locations. This assumption is questionable in studies with smartphone applications, including the Smoke Sense Initiative, where the smoke exposure, study participant’s motivations, and treatment vary across a large, socially, and environmentally diverse domain. It is likely that the treatment effect varies across spatial locations. Although spatially varying coefficient models exist (e.g., Gelfand et al., 2003), they restrict to study the associational relationship of treatment and outcome and thus lack causal interpretations. Reich et al. (2021) provided a comprehensive review of spatial causal inference methods and suggested that causal models with spatially varying effects are largely needed.

We establish the causal effect model that allows the causal effect to vary over space accounting for unmeasured spatial treatment effect modifiers. Under the standard sequential randomization assumption, we show that the local causal parameter can be identified based on a class of estimating equations. To borrow information from nearby locations, we adopt the local estimating equation approach via local polynomials (Fan and Gijbels, 1996) and geographical kernel weighting (Fotheringham et al., 2003). Moreover, we also derive the asymptotic theory and propose an easy-to-implement inference procedure based on the wild bootstrap. Within the new framework, a challenge arises for selecting the bandwidth parameter determining the scale of spatial treatment effect heterogeneity. Existing methods rely on cross-validation on predictions, where a typical loss function is the mean squared prediction error, which is not applicable under the causal framework because the task is estimating causal effects rather than predicting outcomes. This is due to the fundamental problem in causal inference that not all ground-truth potential outcomes can be observed (Holland, 1986). We propose a loss function using a new balancing criterion for bandwidth selection. Finally, we propose to use an instrumental variable for the Smoke Sense application that adjusts for informative missingness.

Our analytic framework is appealing for multiple reasons. First, the framework is semiparametric and does not require modeling the full data distribution. Second, it is doubly robust in the sense that, with a correct treatment effect model, the proposed estimator is consistent if either the propensity score model or a nuisance outcome mean model is correctly specified. Third, it is flexible enough to handle informative missingness by inverse probability weighting of estimating functions. Fourth, it is a very general framework of spatially- and time-varying causal effect estimation which has much potential in many other mobile health applications such as diagnostic and treatment support, disease and epidemic outbreak tracking, etc (Adibi, 2014).

The rest of the paper is organized as follows. Section 2 introduces the data sources and notation. Section 3 describes existing global structural nested mean models (SNMMs). Section 4 develops new local SNMMs, local estimation, and the asymptotic properties. We extend the framework to handle informative non-responses with instrument variables in Section 5. We apply the method to the simulated data and real data collected from the Smoke Sense Initiative in Section 6 and Section 7, respectively. We conclude the article with a discussion in Section 8.

2 Smoke Sense citizen science study

The dataset from the Smoke Sense citizen science study combines the self-reported observations of smoke, health symptoms, and behavioral actions taken in response to smoke and the estimated exposure to wildfire smoke recorded by the National Oceanic and Atmospheric Administration’s Office of Satellite and Product Operations Hazard Mapping System’s Smoke Product (HMS).

2.1 Smoke Sense app

The Smoke Sense citizen science study is facilitated through the use of a smartphone application, a publicly available mobile application on the Google Play Store and the Apple App Store. The app invites users to record their smoke observations and health symptoms, as well as the actions they took to protect their health. In the app, participants can also explore current and forecasted daily air quality, learn where the current wildfires are burning (Figure 1), read about the progress of the wildfire suppression efforts, and observe satellite images of smoke plumes. Participants are also invited to play educational trivia games, explore what other users are reporting, learn strategies to minimize exposure, and learn about the health impacts of wildland fire smoke. Participants earn badges for the level of participation as users, observers, learners, and reporters.

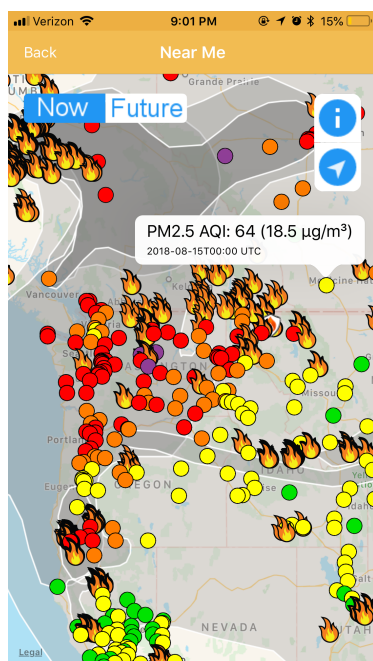


Figure 1: A screen shot of the Smoke Sense App alerting the user of local fires and air quality.

In this study, the outcome of interest is the number of user-reported adverse health symptoms during the 2019 smoke season, reported as weekly summaries. The weekly number of adverse events ranged from 0 to 15 with a mean (sd) of 2.6 (3.2). The treatment is a binary indicator of whether the participant took strong protective behaviors – staying indoors with extra protective behaviors like using an air cleaner or a respirator mask. Other variables include the baseline information when registered in the app including age, gender, first 3-digits of the zip code, etc, and time-varying variables including self-reported smoke experience, days of visibility impacted, etc, which users are reminded of reporting every week. More details about the variables are provided in Supplementary Materials. In our analysis, we include $n = 1882$ users who reported baseline and time-varying variables. Among these users, 471 reported more than once and the maximum number of reporting is 61.

2.2 Wildfire smoke exposure

For each user-week, the exposure to smoke is determined based on HMS (http://satepsanone.nesdis.noaa.gov/pub/volcano/FIRE/HMS_ARCHIVE/). The HMS data contains the spatial contours of satellite observed imagery of smoke together with the estimated density of fine particulate matter ($\text{PM}_{2.5}$) based on the air quality model. The smoke density in the HMS data is summarized by four levels: none, light ($\text{PM}_{2.5}$ range: $0 - 10 \mu\text{g}/\text{m}^3$, medium ($10.5 - 21.5 \mu\text{g}/\text{m}^3$), and dense ($\geq 22 \mu\text{g}/\text{m}^3$), where each level is summarized by the midpoint of the corresponding range ($0, 5, 16,$ and $27 \mu\text{g}/\text{m}^3$, respectively). We map the highest daily exposure value to each zip code and aggregate the HMS data by taking the maximum value over the 3-digit zip code (zip3). We restrict our analysis to the time period from September 2018 to the end of 2019 and across zip3 where there were more than 10 smoke sense users. Figure 2 shows the map of the maximum weekly smoke density across zip3 geographic locations during the study period, where the west coast showed heavier wildland fire smoke occurrence.

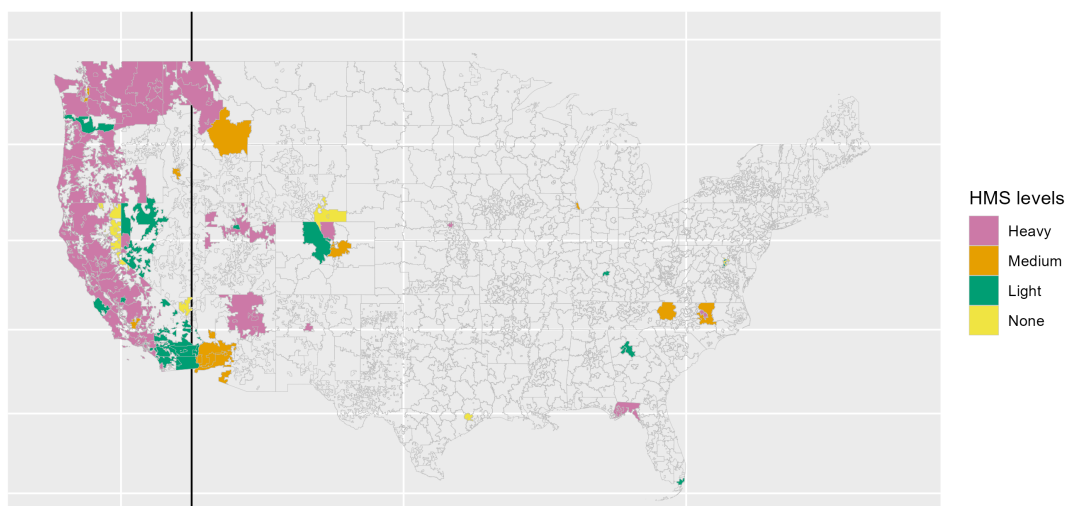


Figure 2: Maximum daily HMS smoke density level in each three-digit zip code over the study period. The smoke density has four levels: None, Light, Medium, and Heavy (corresponding to $0, 5, 16,$ and $27 \mu\text{g}/\text{m}^3$, respectively). The vertical line is at longitude -115 .

2.3 Notation

We follow the notation from the standard structural nested model literature (Robins, 1994). We assume n subjects are monitored over time points t_0, \dots, t_K . For privacy concerns, the spatial location of the subjects are summarized by their 3-digit zip codes. To obtain the latitude and longitude of the spatial location, $\mathbf{s} = (s_1, s_2)$, we average the latitude and longitude coordinates over all the 5-digit zip codes which have the same 3-digit zip codes (the latitude and longitude coordinates corresponding to each 5-digit zip code are available at <https://public.opendatasoft.com/explore/dataset/us-zip-code-latitude-and-longitude/export/>). The subjects are

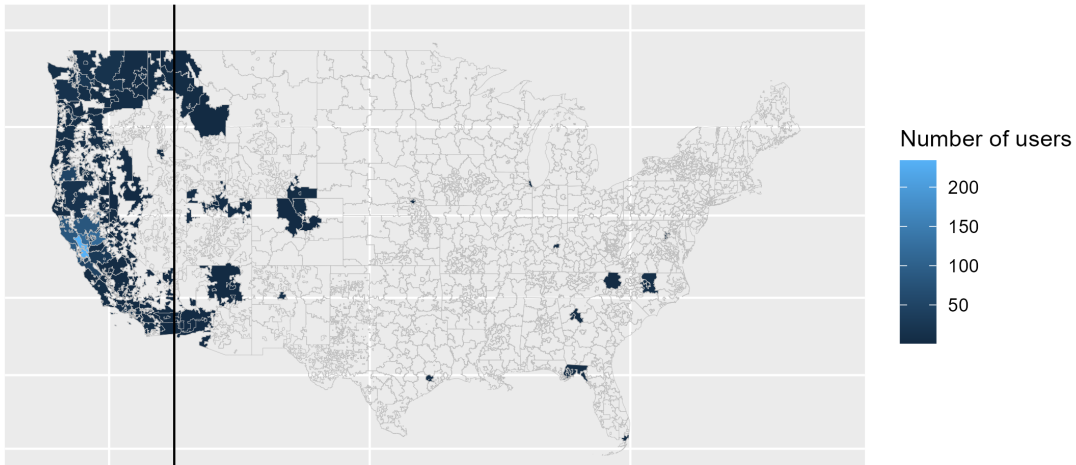


Figure 3: The number of users in each three-digit zip code over the study period. The vertical line is at longitude -115.

assumed to be an independent sample, which is a plausible assumption since the health symptoms in the data are not like infectious disease so that the interference is not likely. And for simplicity, we omit a subscript for subject and location; that is, any variable will have a subject index i and a location index s implicitly. Let A_k be the binary treatment at t_k ($A_k = 1$ if the subject reported taking the strong protective behaviors, and $A_k = 0$ if the subject did not take any behavior or took some mild protective behaviors). Let X_0 be a vector of baseline variables, including the subject’s demographic information (e.g., sex, age, race, education level), baseline health information (e.g., pre-existing conditions, physical activity level, time spent outdoors), and current beliefs about smoke and air pollution. Let $X_k \in \mathcal{X}_k$ be a vector of baseline covariates and time-varying variables at t_k (e.g., the recent experience of smoke, feeling status, visibility). Let Y_k be the outcome at t_k (the total number of symptoms the subject had including e.g. anxiety, asthma attack, chest pain).

We use overbars to denote a variable’s history; e.g., $\bar{A}_k = \{A_m : m = 0, \dots, k\}$, and the complete history \bar{A}_K abbreviates to \bar{A} . Let $Y_k^{(\bar{a})}$ be the outcome at t_k , possibly counterfactual, had the subject followed treatment regime \bar{a} over the study period from t_0 to t_K . For simplicity, we use $Y_k^{(\bar{a}_m)}$ ($m \leq k$) to denote the potential outcome at t_k had the subject followed treatment regime \bar{a}_m until t_m and no treatment onwards. We assume that the observed outcome Y_k is equal to $Y_k^{(\bar{A})}$ for $k = 0, \dots, K$ as different strong protective behaviors considered in our study presumably reduce exposure to smoke or harmful air to a similar extent. Finally, $V = (\bar{A}, \bar{X}, \bar{Y})$ denotes the subject’s full records. Up to Section 5, we shall assume that all subjects’ full records are observed. We let \mathbb{P} be the probability measure induced by V and \mathbb{P}_n be the empirical measure for V_1, \dots, V_n ; i.e., $\mathbb{P}_n f(V) = n^{-1} \sum_{i=1}^n f(V_i)$ for any real-valued function $f(v)$.

3 Global structural nested mean models

The treatment effect is defined in terms of the expected value of potential outcomes under different treatment trajectories. Because both the treatment and outcome are longitudinal, and

there may be a lag time between the treatment and its effect, we define the causal effect of the treatment at t_m on the outcome at t_k for $k \geq m$. SNMMs are one type of causal models designed to properly handle such time-varying treatments and confounders. We have provided additional details using a *directed acyclic graph* (DAG) in the Supplementary Material to illustrate their ability to capture time-varying treatment effects, as compared to standard regression models.

Definition 1 (Global SNMM) Let \bar{a}_{-1} denote a null set by convention, and $\gamma_{m,k}(\psi^*) = \gamma_{m,k}(\bar{a}_m, \bar{x}_m; \psi^*)$ be a known function of (\bar{a}_m, \bar{x}_m) with a vector of unknown parameters $\psi^* \in \mathcal{R}^p$ with a fixed $p \geq 1$. For $0 \leq m \leq k \leq K$, the treatment effect is characterized by

$$E \left\{ Y_k^{(\bar{a}_{m-1}, a_m)} - Y_k^{(\bar{a}_{m-1}, 0)} \mid \bar{A}_{m-1} = \bar{a}_{m-1}, \bar{X}_m = \bar{x}_m \right\} = \gamma_{m,k}(\psi^*), \quad (1)$$

where the causal effect is the expected difference in the response at t_k between two counterfactual regimes with the same treatment before t_m , different treatment at t_m , and no treatments after t_m .

To help understand the model, consider the following example.

Example 1 Assume $\gamma_{m,k}(\psi^*) = \delta \exp \left\{ -(t_k - t_m - \mu)^2 / (2\sigma^2) \right\} a_m$, where $\psi^* = (\delta, \mu, \sigma^2)$ is the vector of parameters.

This model entails a key feature for the treatment effect curve: the effect of treatment a_m on future health outcomes increases smoothly over time, reaches to a peak effect δ after μ units of time, and decreases to zero as time further increases. The rationale behind this delayed effect pattern is that taking protective behaviors may not lead to immediate changes in health outcomes. Therefore, the impact on the total number of adverse health symptoms is anticipated to peak after a certain duration and gradually decrease to zero for large time lags.

This framework can also include effect modifiers. For example, we can consider $\gamma_{m,k}(\psi^*) = a_m(1, x_m^T) \psi^*$, where x_m is a $(p-1)$ -vector of the individual characteristics and $\psi^* = (\psi_1^*, \dots, \psi_p^*)^T$. Therefore, the class of SNMMs has important applications in precision medicine (Chakraborty and Moodie, 2013) for the discovery of optimal treatment regimes that are tailored to individuals' characteristics and environments.

Parameter identification requires the typical sequential randomization assumption (Robins et al., 1992) that for $0 \leq m \leq k \leq K$, $Y_k^{(\bar{a}_m)} \perp\!\!\!\perp A_m \mid \bar{L}_m$, where $\bar{L}_m = (\bar{A}_{m-1}, \bar{X}_m, \bar{Y}_{m-1})$. This assumption holds if \bar{L}_m captures all confounders for the treatment at t_m and ensuing outcomes. Define the propensity score as $e(\bar{L}_m) = P(A_m = 1 \mid \bar{L}_m)$. Moreover, define $H_k^{(\bar{A}_{m-1})}(\psi^*) = Y_k - \sum_{l=m}^k \gamma_{l,k}(\psi^*)$ and $\mu_{m,k}(\bar{L}_m) = E\{H_k^{(\bar{A}_{m-1})}(\psi) \mid \bar{L}_m\}$. Intuitively, $H_k^{(\bar{A}_{m-1})}(\psi^*)$ removes the accumulated treatment effects from t_m to t_k from the observed outcome Y_k , so it mimics the potential outcome $Y_k^{(\bar{a}_{m-1})}$ had the subject followed $\bar{a}_{m-1} = \bar{A}_{m-1}$ but no treatment onwards. The sequential randomization assumption states that $Y_k^{(\bar{a}_{m-1})}$ and A_m are independent given \bar{L}_m . Robins et al. (1992) showed that $H_k^{(\bar{A}_{m-1})}(\psi^*)$ inherits this property in the sense that $E\{H_k^{(\bar{A}_{m-1})}(\psi) \mid A_m, \bar{L}_m\} = E\{H_k^{(\bar{A}_{m-1})}(\psi) \mid \bar{L}_m\}$. As a result, with any measurable, bounded function $q_{k,m} : \bar{L}_m \rightarrow \mathcal{R}^p$,

$$G(V; \psi) = \sum_{m=1}^K \sum_{k=m}^K q_{k,m}(\bar{L}_m) \left\{ H_k^{(\bar{A}_{m-1})}(\psi) - \mu_{m,k}(\bar{L}_m) \right\} \{A_m - e(\bar{L}_m)\} \quad (2)$$

is unbiased at ψ^* . Then, under a regularity condition that $E\{\partial G(V; \psi) / \partial \psi\}$ is invertible, the solution to $E\{G(V; \psi)\} = 0$ uniquely exists, and therefore ψ^* is identifiable.

The estimating function $G(V; \psi)$ depends on $q_{k,m}(\bar{L}_m)$. The choice of $q_{k,m}(\bar{L}_m)$ does not affect the unbiasedness but estimation efficiency. We adopt an optimal form of $q_{k,m}(\bar{L}_m)$ given in the Supplementary Material. With this choice, the solution to $\mathbb{P}_n G(V; \psi) = 0$ has the smallest asymptotic variance compared to other choices (Robins, 1994).

4 Local structural nested mean model

Global SNMMs in Section 3 allow time-varying treatment effects but not spatially varying treatment effects. That is, the treatment effects for a given time are the same across space. Although the global SNMMs can model the spatial heterogeneity of treatment effects by using the observed spatial covariates, there may be unobserved location-specific heterogeneity. To overcome this issue, we extend to a new class of models that allows modeling spatial treatment effect heterogeneity using spatially local parameters. Specifically, Section 4.1 proposes the spatially varying SNMM to estimate the location-specific treatment effect. Section 4.2 introduces an extension of the location-specific estimating equations by incorporating the neighborhood information through geographically weighted regression. Section 4.3 examines the asymptotic properties of the proposed estimator, and Sections 4.4 to 4.6 offer guidance on tuning the bandwidth, bias correction, and inference in practice.

4.1 Spatially varying structural nested mean models

The local SNMM is formulated by considering a vector of spatially varying parameters, denoted as $\psi^*(\mathbf{s})$, for each location \mathbf{s} in (1).

Definition 2 (Local SNMM) Let $\gamma_{m,k}\{\psi^*(\mathbf{s})\} = \gamma_{m,k}\{\bar{a}_m, \bar{x}_m; \psi^*(\mathbf{s})\}$ be a known function of (\bar{a}_m, \bar{x}_m) with a vector of spatially varying parameters $\psi^*(\mathbf{s}) \in \mathcal{R}^p$ with fixed $p \geq 1$. For $0 \leq m \leq k \leq K$, the treatment effect is characterized by

$$E\left\{Y_k^{(\bar{a}_{m-1}, a_m)} - Y_k^{(\bar{a}_{m-1}, 0)} \mid \bar{A}_{m-1} = \bar{a}_{m-1}, \bar{X}_m = \bar{x}_m\right\} = \gamma_{m,k}\{\psi^*(\mathbf{s})\}, \quad (3)$$

where \mathbf{s} is a fixed location that is implicitly involved in the left-hand side of (3).

Consider the following example in parallel to Example 1.

Example 2 Assume $\gamma_{m,k}\{\psi^*(\mathbf{s})\} = \delta(\mathbf{s}) \exp[-(t_k - t_m - \mu(\mathbf{s}))^2 / \{2\sigma(\mathbf{s})^2\}] a_m$, where \mathbf{s} is a given spatial location.

The local model in Example 2 entails that the treatment would increase the mean of the outcome for subjects at location \mathbf{s} by $\delta(\mathbf{s})$ at its peak when $t_k = t_m + \mu(\mathbf{s})$ if the subject had received the treatment at t_m . The spatial variations in the timing and intensity of peak effects are captured by $\mu(\mathbf{s})$ and $\delta(\mathbf{s})$, which can be attributed to various location-specific heterogeneity.

4.2 Geographically weighted local polynomial estimation

There are an infinite number of parameters because $\psi^*(\mathbf{s})$ varies over \mathbf{s} . Estimation of $\psi^*(\mathbf{s})$ at a given \mathbf{s} may become unstable with only a few observations at \mathbf{s} , or even infeasible at locations without any observations. To make estimation feasible, one can make some global structural assumptions about $\psi^*(\mathbf{s})$ with a fixed number of unknown parameters. However, this approach is sensitive to model misspecification. To overcome this difficulty, we combine the ideas of local polynomial approximation and geographically weighted regression. That is, we leave the global

structure of $\psi^*(\mathbf{s})$ unspecified but approximate $\psi^*(\mathbf{s})$ locally by polynomials of \mathbf{s} . Then, we use geographical weighting to estimate the local parameters by pooling nearby observations whose contributions diminish with geographical distance.

To be specific, we consider estimating $\psi^*(\mathbf{s}^*)$ at a given \mathbf{s}^* . We approximate $\psi^*(\mathbf{s}) = \{\psi_1^*(\mathbf{s}), \dots, \psi_p^*(\mathbf{s})\}^\top$ in the neighborhood of \mathbf{s}^* by the first-order local polynomial,

$$\tilde{\psi}_{1p}(\mathbf{s}; \phi) = \begin{pmatrix} \phi_1^\top d(\mathbf{s}^* - \mathbf{s}) \\ \vdots \\ \phi_p^\top d(\mathbf{s}^* - \mathbf{s}) \end{pmatrix}_{p \times 1}, \quad \phi_j = \begin{pmatrix} \phi_{j,0} \\ \phi_{j,1} \\ \phi_{j,2} \end{pmatrix}_{3 \times 1}, \quad d(\mathbf{s}^* - \mathbf{s}) = \begin{pmatrix} 1 \\ s_1^* - s_1 \\ s_2^* - s_2 \end{pmatrix}_{3 \times 1},$$

and $\phi = (\phi_{1,0}, \dots, \phi_{p,0}, \phi_{1,1}, \dots, \phi_{p,1}, \phi_{1,2}, \dots, \phi_{p,2})^\top$ is the vector of unknown coefficients. Although we use the first-order local polynomial approximation, extensions to higher-order approximations are straightforward with heavier notation. As established in Section 2, $\psi^*(\mathbf{s}^*)$ is identified based on the estimating function (2), so we adopt the local estimating equation approach (Carroll et al., 1998) with geographical weighting. We propose a geographically weighted estimator $\hat{\phi}_\tau(\mathbf{s}^*)$ by solving

$$\begin{aligned} & \mathbb{P}_n \left[\omega_\tau(\|\mathbf{s}^* - \mathbf{s}\|) d(\mathbf{s}^* - \mathbf{s}) \otimes G\{V; \tilde{\psi}_{1p}(\mathbf{s}; \phi, \mu, e)\} \right], \\ & = \mathbb{P}_n \left\{ \omega_\tau(\|\mathbf{s}^* - \mathbf{s}\|) \begin{pmatrix} 1 \\ s_1^* - s_1 \\ s_2^* - s_2 \end{pmatrix} \right. \\ & \left. \otimes \left(\sum_{m=1}^K \sum_{k=m}^K q_{k,m}(\bar{L}_m) \left[H_k^{(\bar{A}_{m-1})} \{\tilde{\psi}_{1p}(\mathbf{s}; \phi)\} - \mu_{m,k}(\bar{L}_m) \right] \{A_m - e(\bar{L}_m)\} \right) \right\} = 0, \end{aligned} \quad (4)$$

for ϕ , where $M_1 \otimes M_2$ denotes the Kronecker product of M_1 and M_2 , $H_k^{(\bar{A}_{m-1})} \{\tilde{\psi}_{1p}(\mathbf{s}; \phi)\} = Y_k - \sum_{l=m}^k \gamma_{l,k} \{\tilde{\psi}_{1p}(\mathbf{s}; \phi)\}$, and $\omega_\tau(\cdot)$ is a spatial kernel function with a scale parameter τ . The first p -vector $\hat{\phi}_{\tau,0}(\mathbf{s}^*)$ in $\hat{\phi}_\tau(\mathbf{s}^*)$ estimates $\psi^*(\mathbf{s}^*)$. The estimating equation (4) assigns more weight to observations nearby than those far from the location \mathbf{s}^* . The commonly-used weight function is $\omega_\tau(\|\mathbf{s}^* - \mathbf{s}\|) = \tau^{-1} K\{\|\mathbf{s}^* - \mathbf{s}\|/\tau\}$, where $K(\cdot)$ is the Gaussian kernel density function. The scale parameter τ is the bandwidth determining the scale of spatial treatment effect heterogeneity; $\psi^*(\mathbf{s})$ is smooth over \mathbf{s} when τ is large, and vice versa.

We illustrate the geographically weighted estimator of $\psi^*(\mathbf{s}^*)$ with a simple example, which allows an analytical form.

Example 3 For the spatially varying structural nested mean model in Example 2, the geographically weighted estimator of $\psi^*(\mathbf{s}^*)$ is the first p -vector of $\hat{\phi}_\tau(\mathbf{s}^*)$ solving (4), with $\gamma_{m,k} \{\tilde{\psi}_{1p}(\mathbf{s}; \phi)\} = \delta_{1p}(\mathbf{s}; \phi) \exp[-\{t_k - t_m - \mu_{1p}(\mathbf{s}; \phi)\}^2 / \{2\sigma_{1p}(\mathbf{s}; \phi)^2\}] a_m$, where

$$\begin{aligned} \delta_{1p}(\mathbf{s}; \phi) &= \delta + \phi_{1,1}(s_1^* - s_1) + \phi_{1,2}(s_2^* - s_2), \\ \mu_{1p}(\mathbf{s}; \phi) &= \mu + \phi_{2,1}(s_1^* - s_1) + \phi_{2,2}(s_2^* - s_2), \\ \sigma_{1p}(\mathbf{s}; \phi)^2 &= \sigma^2 + \phi_{3,1}(s_1^* - s_1) + \phi_{3,2}(s_2^* - s_2), \end{aligned}$$

and $\phi = (\delta, \mu, \sigma^2, \phi_{1,1}, \phi_{2,1}, \phi_{3,1}, \phi_{1,2}, \phi_{2,2}, \phi_{3,2})$.

Remark 1 It is worth discussing an alternative way to approximate $\mu_{m,k}(\bar{L}_m)$ by noticing that $\mu_{m,k}(\bar{L}_m) = E\{Y_k^{(\bar{A}_{m-1})} \mid \bar{L}_m\}$. It amounts to identifying subjects who followed a treatment regime $(\bar{A}_{m-1}, \bar{0})$ and fitting the outcome mean model based on Y_k and \bar{L}_m among these subjects.

4.3 Asymptotic properties

We show that the proposed estimator has an appealing double robustness property in the sense that the consistency property requires that one of the nuisance function models is correctly specified, not necessarily both. This property adds protection against possible misspecification of the nuisance models. Below, we establish the asymptotic properties of $\hat{\phi}_{\tau,0}(\mathbf{s}^*)$, including robustness, asymptotic bias and variance. Assume the observed locations are continuously distributed over a compact study region. Let $f_{\mathbf{s}}(\mathbf{s})$ be the marginal density of the observed locations \mathbf{s} , which is bounded away from zero. Also, assume that $\psi(\mathbf{s})$ is twice differentiable with bounded derivatives. The kernel function $K(\cdot)$ is bounded and symmetric, and the bandwidth satisfies $\tau \rightarrow 0$ and $n\tau^2 \rightarrow \infty$ as $n \rightarrow \infty$.

Theorem 1 *Suppose Assumption 1, the sequential randomization assumption and the regularity conditions presented in the Supplementary Material hold. Let $\hat{\phi}_{\tau}(\mathbf{s}^*)$ be the solution to (4) with $\mu_{m,k}(\bar{L}_m)$ and $e(\bar{L}_m)$ replaced by their estimates $\hat{\mu}_{m,k}(\bar{L}_m)$ and $\hat{e}(\bar{L}_m)$. Let $\hat{\phi}_{\tau,0}(\mathbf{s}^*) = e_1^{\top} \hat{\phi}_{\tau}(\mathbf{s}^*)$, where $e_1 = (I_{p \times p}, 0_{p \times p}, 0_{p \times p})^{\top}$. If either $\mu_{m,k}(\bar{L}_m)$ or $e(\bar{L}_m)$ is correctly specified, $\hat{\phi}_{\tau,0}(\mathbf{s}^*)$ is consistent for $\psi^*(\mathbf{s}^*)$, and*

$$\{n\tau^2 f_{\mathbf{s}}(\mathbf{s}^*)\}^{-1/2} \left\{ \hat{\phi}_{\tau,0}(\mathbf{s}^*) - \psi^*(\mathbf{s}^*) - \tau^2 \mathcal{G}_b(\mathbf{s}^*) \right\} \rightarrow \mathcal{N}\{0_{p \times 1}, \mathcal{G}_v(\mathbf{s}^*)\},$$

where $\mathcal{G}_b\{\mathbf{s}^*, K, \psi(\mathbf{s}^*)\}$ and $\mathcal{G}_v\{\mathbf{s}^*, K, \psi(\mathbf{s}^*)\}$ do not depend on τ .

The proof and the expressions of $\mathcal{G}_b\{\mathbf{s}^*, K, \psi(\mathbf{s}^*)\}$ and $\mathcal{G}_v\{\mathbf{s}^*, K, \psi(\mathbf{s}^*)\}$ are presented in the Supplementary Material.

4.4 Bandwidth selection using a balancing criterion

We use the K-fold cross-validation to select the bandwidth τ . An important question arises about the loss function. We propose a new objective function using a balancing criterion. The key insight is that with a good choice of τ , the mimicking potential outcome $H_k^{(\bar{A}_m-1)}\{\hat{\phi}_{\tau,0}(\mathbf{s}^*)\}$ is approximately uncorrelated to A_m given \bar{L}_m ; therefore, the distribution of $H_k^{(\bar{A}_m-1)}\{\hat{\phi}_{\tau,0}(\mathbf{s}^*)\}$ is balanced between $A_m = 1$ and $A_m = 0$ among the group with the same \bar{L}_m . If \bar{L}_m contains continuous variables, the balance measure is difficult to formulate because it involves forming subgroups by collapsing observations with similar values of \bar{L}_m . To avoid this issue, inspired by the estimating functions, we formulate the loss function as

$$G_{\text{loss}}\{V; \psi(\mathbf{s}^*)\} = \left| \mathbb{P}_n \omega_{\tau}(\|\mathbf{s}^* - \mathbf{s}\|) \times \sum_{m=1}^K \sum_{k=m}^K \left[H_k^{(\bar{A}_m-1)}\{\hat{\phi}_{\tau,0}(\mathbf{s}^*)\} - \hat{\mu}_{m,k}(\bar{L}_m) \right] \{A_m - \hat{e}(\bar{L}_m)\} \right|. \quad (5)$$

If τ is too small, $\hat{\phi}_{\tau,0}(\mathbf{s}^*)$ has a large variance and also $\omega_{\tau}(\|\mathbf{s}^* - \mathbf{s}\|)$ is only nontrivial for few locations in the τ -neighborhood of \mathbf{s}^* , which leads to a large value of $G_{\text{loss}}\{V; \psi(\mathbf{s}^*)\}$; while if τ is too large, $\hat{\phi}_{\tau,0}(\mathbf{s}^*)$ has a large bias, which translates to a large loss too. Therefore, a good choice of τ balances the trade-off between variance and bias.

4.5 Bias correction

Theorem 1 provides the asymptotic bias formula, which however involves derivatives of $\psi^*(\mathbf{s}^*)$ and is difficult to approximate. Following Ruppert (1997), we extend the empirical bias correction method to the geographically weighted framework. For a fixed location \mathbf{s}^* , we calculate $\hat{\phi}_{\tau,0}(\mathbf{s}^*)$ at a series of τ over a pre-specified range $\mathcal{T} = \{\tau_1, \dots, \tau_L\}$, where L is at least 3. Based on Theorem 1, the bias function of $\hat{\phi}_{\tau,0}(\mathbf{s}^*)$, with respect to τ , is of order τ^2 . This motivates a bias function of a form $b(\tau; \nu) = \nu_1 \tau^2 + \dots + \nu_q \tau^q$, where q is an integer greater than 2 and $\nu = (\nu_1, \dots, \nu_q)^\top$ is a vector of unknown coefficients. Based on the pseudo data $\{\tau, \hat{\phi}_{\tau,0}(\mathbf{s}^*) : \tau \in \mathcal{T}\}$, fit a function $E\{\hat{\phi}_{\tau,0}(\mathbf{s}^*)\} = \nu_0 + b(\tau; \nu)$ to obtain $\hat{\nu}$. Then, we estimate the bias of $\hat{\phi}_{\tau,0}(\mathbf{s}^*)$ by $b(\tau; \hat{\nu})$. The debiased estimator is $\hat{\phi}_{\tau,0}^{\text{bc}}(\mathbf{s}^*) = \hat{\phi}_{\tau,0}(\mathbf{s}^*) - b(\tau; \hat{\nu})$.

4.6 Wild bootstrap inference

For variance estimation, Carroll et al. (1998) proposed using the sandwich formula in line with the Z-estimation literature. The sandwich formula is justified based on asymptotics. To improve the finite-sample performance, Galindo et al. (2001) proposed a bootstrap inference procedure for local estimating equations. However, this procedure involves constructing complicated residuals and a heuristic modification factor. Thus, we suggest an easy-to-implement wild bootstrap method for variance estimation of $\hat{\phi}_{\tau,0}^{\text{bc}}(\mathbf{s}^*)$.

For each bootstrap replicate, we generate exchangeable random weights ξ_i ($i = 1, \dots, n$) independent and identically distributed from a distribution that has mean one, variance one and is independent of the data; e.g., $\text{Exp}(1)$. The regular nonparametric bootstrap is included as a special case by adopting the multinomial distribution to generate the weights. Repeat the cross-validation for choosing τ , calculation of $\hat{\phi}_{\tau,0}(\mathbf{s}^*)$, and bias-correction steps but all steps are carried out using weighted analysis with ξ_i for subject i . Importantly, we do not need to re-estimate the nuisance functions for each bootstrap replication, because they converge faster than the geographically weighted estimator. This feature can largely reduce the computational burden in practice. The variance estimate $\hat{V}(\mathbf{s}^*)$ of $\hat{\phi}_{\tau,0}^{\text{bc}}(\mathbf{s}^*)$ is the empirical variance of a large number of bootstrap replicates. With the variance estimate, we can construct the Wald-type confidence interval as $\hat{\phi}_{\tau,0}^{\text{bc}}(\mathbf{s}^*) \pm z_{1-\alpha/2} \left\{ \hat{V}(\mathbf{s}^*) \right\}^{1/2}$.

5 Extension to the settings with non-responses

In large longitudinal observational studies, non-responses are ubiquitous. To accommodate non-responses, let $\bar{R} = (R_0, \dots, R_K)$ be the vector of response indicators; i.e., $R_m = 1$ if the subject responded at t_m and 0 otherwise. With a slight abuse of notation, let $V = (\bar{A}, \bar{X}, \bar{Y}, \bar{R})$ be the full data. Let $\pi_m(V) = P(R_m = 1 \mid V)$ be the response probability at t_m . If the response probabilities are known, an inverse probability weighted (IPW) estimating function

$$G_{\text{ipw}}\{V; \psi(\mathbf{s})\} = \sum_{m=1}^K \left\{ \sum_{k=m}^K \omega_{m:k}(\bar{R}) q_{k,m}(\bar{L}_m) \left[H_k^{(\bar{A}_{m-1})} \{ \psi(\mathbf{s}) \} - \mu_{m,k}(\bar{L}_m) \right] \right\} \times \{A_m - e(\bar{L}_m)\}, \quad (6)$$

is unbiased at $\psi^*(\mathbf{s})$, where $\omega_{m:k}(\bar{R}) = \prod_{l=m}^k \{R_l \pi_l(V)^{-1}\}$ is the inverse probability weights of responding from t_m to t_k . The geographically weighted local polynomial framework applies by using (6) for estimating $\psi^*(\mathbf{s}^*)$.

In practice, $\pi_m(V)$ is unknown. We require further assumptions for identification and estimation of $\pi_m(V)$. The most common approach makes a missingness at random assumption (Rubin, 1976) that $\pi_m(V)$ depends only on the observed data but not the missing values. In smartphone applications with subject-initiated reporting, whether subjects reported or not is likely to depend on their current status. Then, the response mechanism depends on the possibly missing values themselves, leading to an informative non-response mechanism. In these settings, one can utilize a non-response instrument to help identification and estimation of $\pi_m(V)$ (Wang et al., 2014; Li et al., 2020). For illustration, we assume a simple informative response mechanism that $\pi_m(V) = \pi(V_m)$, where $V_m = (A_m, X_m, Y_m, \bar{R}_{m-1})$; i.e., $\pi_m(V)$ depends only on the current (possibly missing) status (A_m, X_m, Y_m) and the number of historical responses. Extension to more complicated mechanisms is possible at the expense of heavier notation. We then posit a parametric response model, denoted by $\pi_m(V_m; \eta^*)$ with an unknown parameter $\eta^* \in \mathcal{R}^d$. For informative non-responses, the parameter η^* is not identifiable even with a parametric model (Wang et al., 2014). We assume that there exists an auxiliary variable Z_m called a non-response instrument that can be excluded from the non-response probability, but are associated with the current status even when other covariates are conditioned (see Condition C1 in Theorem 1 of Wang et al., 2014 for the formal definition). Existence of such non-response instruments depends on the study context and available data. For example, in the Smoke Sense initiative, a valid non-response instrument is the smoke plume data HMS measured at monitors, which is related to the subject’s variables but is unrelated to whether the subject reporting or not after controlling for subject’s own perceptions about risk.

With a valid instrument, η^* is identifiable. Following Robins and Rotnitzky (1997), $\hat{\eta}$ can be obtained by solving

$$\mathbb{P}_n \sum_{m=0}^K \left\{ \frac{R_m}{\pi_m(V_m; \eta)} - 1 \right\} h(Z_m, \bar{R}_{m-1}) = 0, \quad (7)$$

where $h(Z_m, \bar{R}_{m-1}) \in \mathcal{R}^d$ is a function of (Z_m, \bar{R}_{m-1}) . An additional complication involves estimating the nuisance functions $\mu_{m,k}(\bar{L}_m)$ and $e(\bar{L}_m)$ in the presence of non-response, which now requires weighting similar to that in (6). The IPW approach requires an accurate model for response probability. Following Yang (2022) and Coulombe and Yang (2024), future work could enhance robustness against model misspecification. We leave this for future research. We summarize the stepwise procedures to obtain the proposed estimator under informative missingness in Algorithm 1, and defer the technical details to the Supplementary Material.

6 Simulation study

We evaluate the finite-sample performance of the proposed estimator on simulated datasets to evaluate the double robustness property. We first consider the simpler case without non-responses in Section 6.1 and then consider the case with non-responses in Section 6.2 to mimic the Smoke Sense data. All codes are parallelized and executed on a computer with Intel(R) Core(TM) i7-8565U CPU, 16 RAM computer. The proposed geographically weighted estimation takes approximately 8 hours when evaluated on a 10×10 grid of spatial locations for one replicated dataset in our simulation study.

6.1 Complete data without non-responses

In this section, we simulate 500 datasets without non-response. In each dataset, we generate n locations. For each location, each subject are associated with P covariates and the subject’s p -th covariate process over $K = 25$ weeks follows a Gaussian process with mean 0, variance 0.5 and a

Algorithm 1: Geographically weighted local polynomial estimation for structural nested mean models

Input: Subjects' full records $V = (A_m, X_m, Y_m)_{m=0}^K$, their spatial locations $\mathbf{s} = (s_1, s_2)$, the grid for selecting τ , the polynomial order q for modeling the bias function, and the bootstrap size B .

Step 1. Fit a response probability model $\hat{\pi}_m(V)$ via (7).

Step 2. Fit a propensity score model $\hat{e}(\bar{L}_m)$ by solving

$$\mathbb{P}_n \left[\sum_{m=0}^K R_m \hat{\pi}_m^{-1}(V) \{A_m e^{-1}(\bar{L}_m) - 1\} h(\bar{L}_m) \right] = 0. \quad (8)$$

Step 3. For each location \mathbf{s}^* , obtain a initial estimator $\hat{\phi}_\tau^{[0]}(\mathbf{s}^*)$ by solving (4) with $G\{V; \tilde{\psi}_{1p}(\mathbf{s}; \phi)\}$ replaced by $G_{\text{ipw}}\{V; \tilde{\psi}_{1p}(\mathbf{s}; \phi)\}$ in (6), where $\phi_\tau^{[0]}(\mathbf{s}^*)$ is the first p -vector in $\tilde{\psi}_{1p}(\mathbf{s}; \phi)$.

Step 4. Using the pseudo outcome $H_k^{(\bar{A}_{m-1})} \{ \hat{\phi}_{\tau,0}^{[0]}(\mathbf{s}^*) \}$ and \bar{L}_m , fit an outcome mean model $\hat{\mu}_{m,k}(\bar{L}_m)$ using the IPW estimating equation.

Step 5. Obtain $\hat{\phi}_{\tau,0}(\mathbf{s}^*)$ by solving the IPW version of (4) with $\hat{e}(\bar{L}_m)$ and $\hat{\mu}_{m,k}(\bar{L}_m)$.

Step 6. The debiased estimator $\hat{\phi}_{\tau,0}^{\text{bc}}(\mathbf{s}^*) = \hat{\phi}_{\tau,0}(\mathbf{s}^*) - b(\tau; \hat{\nu})$ with $\hat{\nu}$ fitted by polynomial regression with order q .

Repeat Steps 1-6 for B times with random weights $\xi_i (i = 1, \dots, n)$ to compute \mathbb{P}_n , and obtain the empirical variance $\hat{V}(\mathbf{s}^*)$ of the bootstrap replicates.

Output: A debiased local geographical kernel weighting estimator $\hat{\phi}_{\tau,0}^{\text{bc}}(\mathbf{s}^*)$ and its confidence interval $\hat{\phi}_{\tau,0}^{\text{bc}}(\mathbf{s}^*) \pm z_{1-\alpha/2} \left\{ \hat{V}(\mathbf{s}^*) \right\}^{1/2}$.

first-order autocorrelation structure with lag-1 correlation 0.5 for $p = 1, \dots, P$. We generate the potential outcome process as $Y_k^{(0)} = \sum_{p=1}^P X_{p,k} + \epsilon_k$, for $k = 1, \dots, K$, where $X_{p,k}$ is the subject's p -th covariate at time t_k , and $\bar{\epsilon}$ follows a Gaussian process with mean 0, variance 0.25, and a first-order autocorrelation structure with lag-1 correlation 0.25. We generate the treatment process as \bar{A} , where $A_k \sim \text{Binomial}\{e(\bar{L}_k)\}$ with $\text{logit}\{e(\bar{L}_k)\} = -1 + 0.5 \sum_{p=1}^P X_{p,k} + 0.25 \text{cum}(\bar{A}_{k-1})$ and $\text{cum}(\bar{A}_{k-1}) = \sum_{m=0}^{k-1} A_m$. The observed outcome process is $Y_k = Y_k^{(0)} + \sum_{m=0}^{k-1} \gamma_{m,k} \{\psi^*(\mathbf{s})\}$, where $\gamma_{m,k} \{\psi^*(\mathbf{s})\} = \psi^*(\mathbf{s}) A_m$, if $k = m + 1$ and zero otherwise. We consider three treatment effect specifications for location $\mathbf{s} = (s_1, s_2)$. In the first two scenarios, $n = 1076$ locations are uniformly sampled over a unit square with $P = 1$. In the third scenario, we consider a similar dimension of covariates as the Smoke Sense data with $P = 25$ and an unobserved spatial covariate Z in an irregular grid. For a given location $\mathbf{s}^* = (s_1^*, s_2^*)$, we generate another covariate process $\bar{Z}_K = (Z_1, \dots, Z_K)^\top$ from a Gaussian process with mean $\mu_Z(s_1, s_2) = \sqrt{s_1^2 + s_2^2}/100$, variance 0.5 and a first-order autocorrelation structure with lag-1 correlation 0.5; and the treatment effect $\gamma_{m,k} \{\psi^*(\mathbf{s})\} = Z_m A_m$. In the fitting process, $\{Z_m, m = 1, \dots, K\}$ are merely a set of unobserved realizations of random variables. Thus, the true treatment effect $\psi^*(\mathbf{s})$ should be $\mu_Z(s_1, s_2)$, which is the mean of \bar{Z}_K . Mimicking the spatial dependence in the Smoke Sense data, the data points with size $n = 1882$ are selected spread over an irregular grid.

(S1) $\psi^*(\mathbf{s}) = \exp(s_1 + s_2)$;

(S2) $\psi^*(\mathbf{s}) = \sin\{2(s_1 + 2s_2 - 1)\}$;

(S3) $\psi^*(\mathbf{s}) = \mu_Z(s_1, s_2)$.

We then consider estimating $\psi^*(\mathbf{s}^*)$ at four locations. For (S1) and (S2), $\mathbf{s}^* = (s_1^*, s_2^*)$ and $s_j^* \in \{0.25, 0.75\}$ ($j = 1, 2$). For (S3), the evaluation locations are $\mathbf{s}_1^* = (37.4 - 122.3)$, $\mathbf{s}_2^* = (39.2, -122.3)$, $\mathbf{s}_3^* = (37.4, -120.2)$, and $\mathbf{s}_4^* = (39.2, -120.2)$ whose latitude and longitude degrees are 1/5 and 4/5 quantiles of the latitude and longitude degrees in the real data set.

To investigate the double robustness in Theorem 1, we consider two models for $\mu_{m,k}(\bar{L}_m)$: (a) a correctly specified linear regression model and (b) a misspecified model by setting $\hat{\mu}_{m,k}(\bar{L}_m) = 0$. We also consider two models for $e(\bar{L}_m)$: (a) a correctly specified logistic regression model with predictors X_m and $\text{cum}(\bar{A}_{m-1})$ and (b) a misspecified logistic regression model with predictors X_m^2 and $\text{cum}(\bar{A}_{m-1})^2$. For all estimators, we consider a grid of geometrically spaced values for τ from $\{\exp(0.005), \exp(0.05)\}$ and use 5-fold cross validation in Section 4.4 to choose τ ; see the Supplementary Material for the Monte Carlo average of the selected τ over a grid of spatial locations and additional simulations. The integer q in the bias function is chosen to be 3. We use the wild bootstrap for variance estimation with the bootstrap size 200.

Table 1 reports the simulation results for Scenarios (S1)–(S3), respectively. When either the model for the propensity score or the model for the outcome mean is correctly specified, the proposed estimator has small bias for all treatment effects at all locations across three scenarios. These results confirm the double robustness in Theorem 1. Moreover, under these cases, the wild bootstrap provides variance estimates that are close to the true variances and good coverage rates that are close to the nominal level.

6.2 Informative non-responses

In this section, we generate data with informative non-responses. The data-generating processes are the same as in Section 6.1, except that $P = 1$ for simplicity and a vector of response indicators \bar{R} is generated, where $R_k \sim \text{Binomial}\{\pi_k(Y_k, \bar{R}_{k-1})\}$ with $\text{logit}\{\pi_k(Y_k, \bar{R}_{k-1})\} = -c + 0.5Y_k + 0.25\text{cum}(\bar{R}_{k-1})$, where $c = -1$ for (S1), (S2) and $c = -2$ for (S3). If $R_k = 1$, (A_k, X_k, Y_k) is observed, otherwise only X_k is observed. Thus, X_k is a non-response instrument. We compare the following estimators.

GWLPc1: the geographically weighted local polynomial estimator with the non-response weights setting to a constant 1, which corresponds to the proposed estimator with a misspecified model for the non-response probability;

GWLPipw: the proposed geographically weighted local polynomial estimator with inverse probability of non-response weighting adjustment.

For both estimators, we consider correctly specified models for the outcome mean and propensity score. We use the same cross-validation and wild bootstrap procedures as in Section 6.

Table 2 reports the simulation results with informative non-responses for Scenarios (S1)–(S3). The GWLPc1 estimator without the inverse probability of non-response weighting adjustment is biased, and its coverage rate is off the nominal level, suggesting that informative missingness would lead to biased conclusions. The GWLPipw estimator with proper weighting adjustment has small bias for all locations across all scenarios.

7 Smoke Sense data application

We now apply the new methodology to the Smoke Sense data to estimate heterogeneous effects of protective measures to mitigate the health impact of wildland fire smoke. We follow the

Table 1: Simulation results for complete data. The Monte Carlo average ($\times 10^{-2}$, Est) and variance ($\times 10^{-3}$, Var) of the estimators, variance estimators ($\times 10^{-3}$, Ve), and coverage rate (% Cr) of 95% confidence intervals. The three scenarios (S1)-(S3) are different values of the true spatially varying effect, and the results are reported separately for four fixed locations (\mathbf{s}_1^* - \mathbf{s}_4^*). The methods vary by whether they have the correct model for the outcome mean $\mu_{m,k}(\bar{L}_m)$ and the propensity score $e(\bar{L}_m)$.

		Scenario (S1)				Scenario (S2)				Scenario (S3)			
		\mathbf{s}_1^*	\mathbf{s}_2^*	\mathbf{s}_3^*	\mathbf{s}_4^*	\mathbf{s}_1^*	\mathbf{s}_2^*	\mathbf{s}_3^*	\mathbf{s}_4^*	\mathbf{s}_1^*	\mathbf{s}_2^*	\mathbf{s}_3^*	\mathbf{s}_4
True		164.9	271.8	271.8	448.2	-47.9	47.9	99.7	59.80	127.9	128.4	125.9	126.5
Propensity score model (\checkmark)													
Mean model (\checkmark)	Est	165.8	270.0	270.4	449.6	-47.4	49.0	100.8	57.2	127.8	128.9	125.9	126.7
	Var	18.9	14.6	17.7	18.0	17.0	13.7	16.9	18.1	1.0	1.5	2.4	2.3
	Ve	16.9	16.5	16.8	18.5	17.1	17.0	18.0	19.4	0.8	2.8	1.3	1.9
	Cr	93.2	96.2	94.6	94.8	93.4	95.8	95.0	93.8	95.1	95.2	94.0	94.6
Mean model (\times)	Est	167.4	270.7	270.6	451.8	-45.8	49.9	100.6	59.3	128.6	125.9	123.3	125.0
	Var	36.3	33.8	39.0	35.2	36.9	33.0	37.5	37.6	12.3	40.7	20.1	38.7
	Ve	37.9	36.0	37.0	36.3	37.9	36.4	37.4	38.1	16.7	56.6	28.0	38.7
	Cr	93.6	96.2	95.0	94.4	94.2	95.4	94.8	95.40	95.3	95.6	92.4	97.6
Propensity score model (\times)													
Mean model (\checkmark)	Est	166.0	269.9	270.3	449.9	-47.1	49.0	100.3	57.4	128.1	128.4	126.0	127.1
	Var	19.6	16.3	17.2	19.7	20.8	16.7	16.9	21.1	1.1	4.1	2.1	2.5
	Ve	18.8	17.8	19.0	20.1	18.9	18.1	19.7	20.8	1.2	4.3	2.1	2.9
	Cr	93.6	95.8	94.6	93.8	92.4	95.2	95.6	94.8	95.8	95.6	93.6	96.8
Mean model (\times)	Est	213.5	317.9	317.4	498.1	0.1	96.9	147.7	106.	1467	1465	1472	1470
	Var	38.0	36.3	48.9	33.6	33.9	35.7	48.7	36.0	244	657	469	551
	Ve	37.6	36.3	36.8	37.9	38.0	38.9	38.3	40.3	261	896	447	642
	Cr	22.0	25.0	23.6	24.6	22.6	19.4	22.4	29.0	0.0	0.0	0.0	0.0

\checkmark (is correctly specified), \times (is misspecified)

Table 2: Simulation results for data with informative non-responses. The Monte Carlo average ($\times 10^{-2}$, Est) and variance ($\times 10^{-3}$, Var) of the estimators, variance estimators ($\times 10^{-3}$, Ve), and coverage rate (% Cr) of 95% confidence intervals. The three scenarios (S1)-(S3) are different values of the true spatially varying effect, and the results are reported separately for four fixed locations (\mathbf{s}_1^* - \mathbf{s}_4^*). The methods vary by whether they have the correct (GWLPIPw) or incorrect (GWLPC1) model for the missing data mechanism (π_m).

		Scenario (S1)				Scenario (S2)				Scenario (S3)			
		\mathbf{s}_1^*	\mathbf{s}_2^*	\mathbf{s}_3^*	\mathbf{s}_4^*	\mathbf{s}_1^*	\mathbf{s}_2^*	\mathbf{s}_3^*	\mathbf{s}_4^*	\mathbf{s}_1^*	\mathbf{s}_2^*	\mathbf{s}_3^*	\mathbf{s}_4^*
True		164.9	271.8	271.8	448.2	-47.9	47.9	99.7	59.8	127.9	128.5	125.9	126.5
Missing data model (\checkmark)	Est	163.8	271.0	270.4	450.0	-42.9	52.0	101.3	59.0	127.7	132.6	126.9	128.5
	Var	63.7	43.2	40.4	44.0	148.3	112.4	71.2	91.1	36.6	182.0	46.0	75.5
	Ve	60.5	46.1	46.0	40.5	210.3	123.0	115.5	100.3	33.5	167.5	44.5	78.8
	Cr	93.4	95.4	94.6	92.8	92.2	93.6	94.2	91.8	93.6	94.4	94.4	93.3
Missing data model (\times)	Est	158.2	260.2	260.2	434.0	-45.4	41.1	87.1	48.1	151.6	148.4	148.3	148.6
	Var	44.5	27.9	33.8	29.3	57.8	26.6	24.4	31.9	13.2	81.1	21.0	35.7
	Ve	57.6	29.6	29.7	26.2	70.8	31.5	28.3	44.4	13.6	79.7	20.8	36.3
	Cr	91.4	88.4	86.8	83.0	93.6	93.0	78.0	85.6	46.6	86.8	63.7	75.0

\checkmark (is correctly specified), \times (is misspecified)

basic setup in Section 2, where the data are recorded monthly ($t_k = k$ is the k th month after registration).

To model the treatment effect, a complication arises because taking protective behaviors might not have immediate effects on health outcomes and also the effect on the future outcomes eventually reduces to zero for large time lags. Taking these features into account, we consider the treatment effect model of a squared exponential function of the time lag ($t_k - t_m$) as

$$\gamma_{m,k}(\psi^*) = \delta \exp \left\{ -\frac{(t_k - t_m - \mu)^2}{2\sigma^2} \right\} a_m, \quad (9)$$

where $\psi^* = (\delta, \mu, \sigma^2)$ is the vector of parameters. A negative sign of δ indicates that the treatment is beneficial in reducing the number of adverse health outcomes, a larger magnitude of δ means a larger maximum treatment effect, vice versa, and σ^2 determines the duration of the effect across time lags. We consider fitting a global model (9) in Section 7.1 and a local model with spatially varying $\psi^*(\mathbf{s})$ in Sections 7.2 and 7.3. To assess the fitted nuisance functions and the local treatment effect models, a set of diagnostic analyses are conducted in Section S6.2 of the Supplementary Material. According to the model diagnostic statistics, there is no significant evidence to reject the conditional independence between $Y_k - \sum_{l=m}^k \gamma_{l,k} \{\hat{\psi}^*(\mathbf{s}^*)\} - \hat{\mu}_{m,k}(\bar{L}_m)$ and $A_m - \hat{e}(\bar{L}_m)$ for most selected locations and cities. This suggests that \bar{L}_m adequately captures the confounding variables, and $Y_k - \sum_{l=m}^k \gamma_{l,k} \{\hat{\psi}^*(\mathbf{s}^*)\}$ closely resembles the potential outcome $Y_k^{(\bar{a}_{m-1})}$. Thus, we conclude that the models $\gamma_{m,k} \{\hat{\psi}^*(\mathbf{s}^*)\}$, $\hat{\mu}_{m,k}(\bar{L}_m)$ and $\hat{e}(\bar{L}_m)$ are well-fitted.

For the missing values of the covariates, we impute the missing time-varying variables by carrying forward the last observations, and the missing time-independent variables by mean imputation, i.e., the average and max frequency values to impute the continuous/ordinal variables and categorical variables, respectively. The reason that we employ this imputation strategy is to preserve the assumption of sequential ignorability by avoiding the imputation of missing values based on future observations. Furthermore, our proposed method is evaluated after utilizing multiple imputations to fill in the missing covariates in Section S6.4 of the Supplementary Materials, where the global treatment effects exhibit a similar pattern. It should be noted that the randomness due to the missing covariates is accounted for by re-imputing each bootstrapped dataset in the wild bootstrap procedure.

We adopt the non-response instrument variable approach in Section 5 to adjust for informative non-responses. We assume the response probability $\pi_m(V_m)$ follows a logistic regression with a linear predictor $\eta^T \{ 1 \ A_m \ Y_m \ \text{cum}(\bar{R}_{m-1}) \}$. To identify and estimate η , we use the non-response instrument HMS_m , the true smoke status, which affects the subject's health status but is unrelated to whether the subject reporting or not after controlling for the subject's own perceptions about risk. The estimator of η is obtained by solving the estimating equation (7) with $h(Z_m, \bar{R}_{m-1}) = \{ 1 \ \text{cum}(\bar{R}_{m-1}) \ \text{HMS}_m \ \text{HMS}_m^2 \}^T$. The solution is $\hat{\eta} = (0.04, 0.05, 0.11, 0.14)^T$, indicating that more active participants with worse health outcomes are more likely to report. The proposed estimation (6) requires approximately 10 hours to be completed for a single spatial location of the Smoke Sense data under the treatment effect model (9).

7.1 Global estimation

We first consider fitting a global model and estimate the spatially stationary parameters δ, σ^2 and μ by solving the estimating equation (2), which yields estimates $(\hat{\delta}, \hat{\mu}, \hat{\sigma}^2) = (-0.3, 7.0, 3.0)$. Besides considering the Gaussian distributional-based treatment effect model as (9), for sensitivity analysis, we also tried the Gamma distributional-based model as shown in the Supplementary Materials, which gives a similar pattern.

Figure 4 shows the estimated global treatment effect curve with peak height ($\hat{\delta} = -0.3$ symptoms), peak location ($\hat{\mu} = 7.0$ month), and duration (≈ 1 year). The results suggest a long-lasting effect of taking protective measures in reducing adverse health outcomes. The estimated lag between taking protective measures and the maximum reduction in symptoms is 7.0 months and the estimated reduction in symptoms at this lag is 0.3 symptoms. With the wild bootstrap, the 95% confidence interval for δ is $(-0.5, -0.2)$, and thus the treatment effect is statistically significant. We also conduct a sensitivity analysis with a different $\gamma_{m,k}(\psi^*)$. The results in Section S4.1 in the supplementary material suggest that the conclusions are robust to the functional form of $\gamma_{m,k}(\psi^*)$.

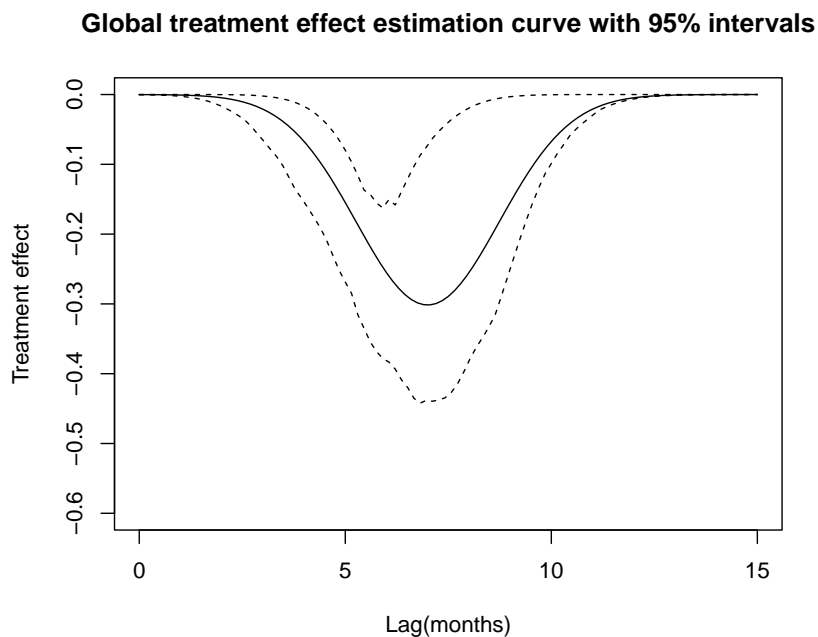


Figure 4: Global treatment effect curve by time lag. The lag ($k - m$) is the time between treatment (at the m th month) and outcome (at the k th month). The solid line is the treatment effect $\gamma_{m,k}(\hat{\psi}^*)$ evaluated at the estimated values $\hat{\psi}^* = (\hat{\delta}, \hat{\mu}, \hat{\sigma}^2) = (-0.3, 7.0, 3.0)$. The dashed lines are the 95% confidence bands constructed from 200 bootstrapped samples.

7.2 Local estimation

The global model assumes the treatment effect curve is the same at all locations. Figure 3 shows that the participants of the Smoke Sense Initiative spread all over the west coast of the US. It is likely that the treatment effect can have spatial heterogeneity due to the large and diverse socially- and environmentally-diverse study domain that is not explained by the observed covariates. In order to investigate the spatially varying treatment effect, we fit a local model using geographical weighting (4). To reduce the computational burden, we use local constant approximation instead of local linear approximation. We choose spatial locations for evaluation as follows. We first set a grid of 56 locations over the west coast of the US; the locations are

combinations of 7 equally-spaced values for the latitude coordinate from 33 to 47 and 8 equally-spaced values for the longitude coordinates from -123 to -115 . Among these locations, we select 28 locations that have samples within the one-degree neighborhood and have more than 0.5% samples within the two-degree neighborhood. Table S4 in the Supplementary Material reports the estimates $\hat{\delta}$, $\hat{\mu}$ and $\hat{\sigma}^2$ and their confidence intervals at the 28 locations, and Figure 5 shows the color map of $\hat{\delta}$. One important finding is that users located in the southwest are more likely to experience significant beneficial treatment effects.

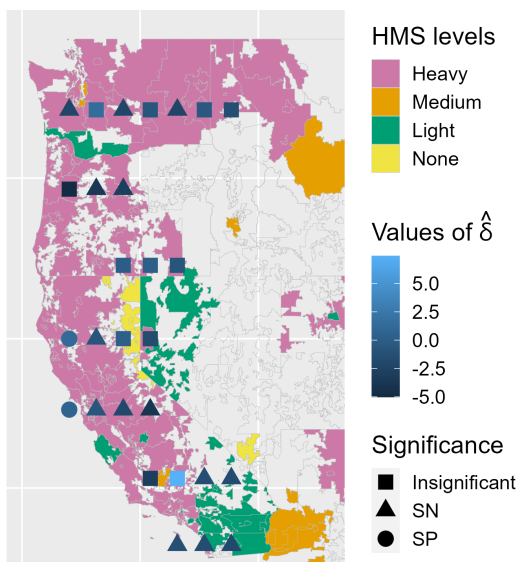


Figure 5: Estimated treatment effect $\hat{\delta}$ for the 28 locations in the Western US. The shapes of symbols denote whether $\hat{\delta}$ is insignificant, significantly negative (SN) or significantly positive (SN). The background color is the maximum daily HMS smoke density in each three-digit zip code. The units of effect is the number of symptoms.

To gain insights into the primary covariates driving the spatial variation in the estimated treatment effect, we consider fitting a random forest model for the estimated treatment effects $\hat{\delta}(\mathbf{s})$ against all the baseline characteristics and two time-varying environmental variables ("Air quality yesterday" and "HMS"). The variable importance, depicted in Figure 6, is arranged based on their impacts in reducing the residual sum of squares. Upon analyzing Figure 6, we observe that "Gender" and "Air quality yesterday" emerge as the two most critical covariates responsible for the spatial variation in the treatment effects. Hence, these two variables play a significant role in explaining the spatial-specific treatment effects.

7.3 Analysis for cities and national parks

We fit the local model to several cities including Spokane, Portland, Seattle, San Diego (SD), San Francisco (SF), Los Angeles (LA), Reno and Las Vegas (LV), as well as prominent national parks including Okanogan-Wenatchee National Forest (OW), Boise, Yosemite National Park (Yosemite), Death Valley National Park (DV), Joshua Tree National Park (Joshua), Lassen National Forest (Lassen). Figure 7 shows a forest plot of the point estimates and confidence

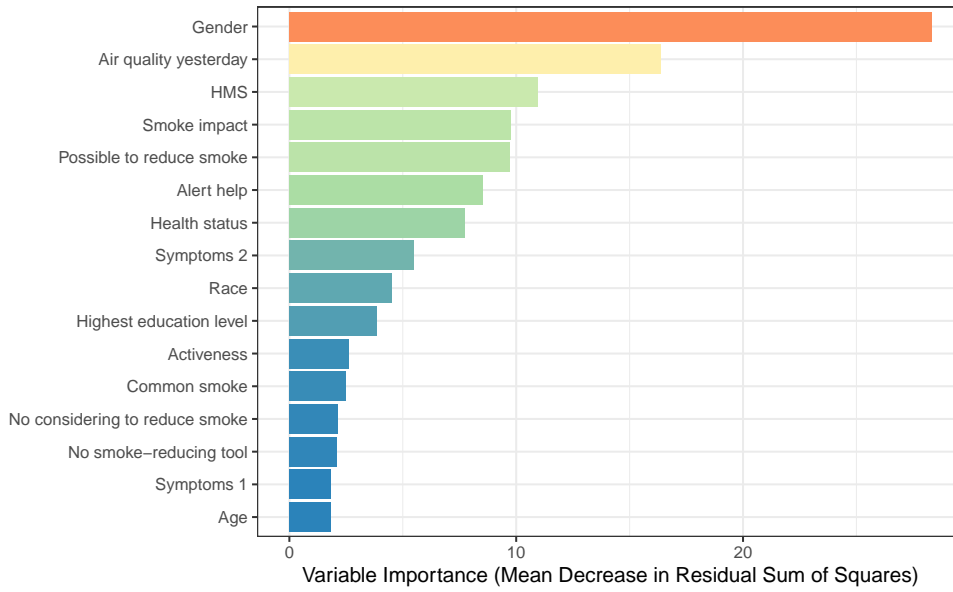


Figure 6: Variable importance plot of the random forest regression model in terms of the mean decrease in residual sum of squares.

intervals for δ . The results align with our discoveries in Section 7.2 that a majority of users in southwest locations (e.g., LA, SD, and Joshua) have significant beneficial treatment effects, whereas such pronounced benefits are uncommon in the northwest. The right panel of Figure 7 provides further evidence with location-specific confidence intervals, confirming the existence of a spatially diverse treatment effect.

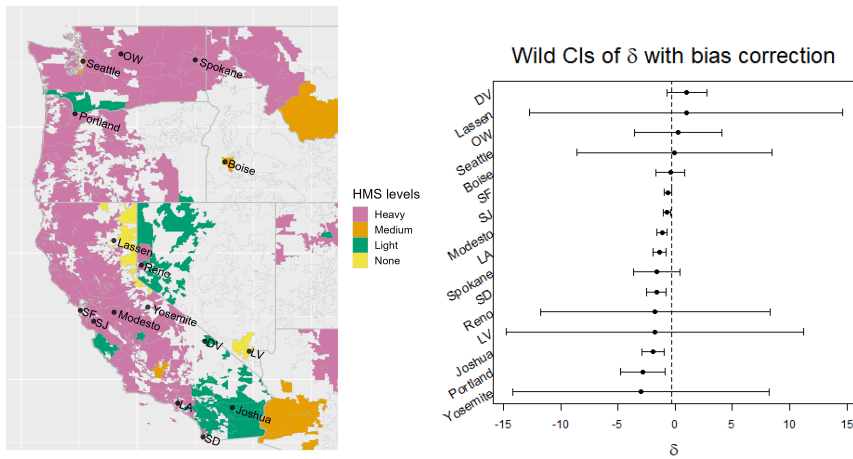


Figure 7: Location (left) and 95% confidence intervals of treatment effects (right) for the selected cities and national parks. The vertical black dash line is the global treatment effect estimate.

8 Discussion

It has become increasingly feasible to evaluate treatment and intervention strategies on public health as more health and activity data are collected via mobile phones, wearable devices, and smartphone applications. We establish a new framework of spatially and time-varying causal effect models. This provides a theoretical foundation to utilize emerging smartphone application data to draw causal inference of interventions on health outcomes. Our approach does not require specifying the full distribution of the covariate, treatment, and outcome processes. Moreover, our method achieves a double robustness property requiring the correct specification of either the model for the outcome mean or the model for the treatment process. The key underpinning assumption is sequential treatment randomization, which holds if all variables are measured that are related to both treatment and outcome. Although essential, it is not verifiable based on the observed data but relies on subject matter experts to assess its plausibility.

The goal of the Smoke Sense citizen science study is to engage the participants on the issue of wildfire smoke as a health risk and facilitate the adaptation of health-protective measures. Our new analysis framework reveals that there is a spatially varying health benefit and that the global model underestimates the treatment effect in areas with the highest exposure to wildland fire smoke. This new knowledge obtained from the spatial analysis may also help Smoke Sense scientists and developers improve the app by targeting different people with different messaging.

There are several directions for future work. First, the study’s conclusion is restricted to Smoke Sense participants and may not apply to the general population. Generalizing these findings to a broader population is an interesting topic, as discussed by Lee et al. (2022), Lee et al. (2023), Lee et al. (2024), and Lee et al. (2024). Second, this work focuses on structural nested “mean” models for continuous or approximately continuous outcomes. It is important to continue the development of local causal models to accommodate different types of outcomes. For example, we can consider the structural nested failure time models for a time-to-event outcome (Yang et al., 2020). Third, the current framework relies on the sequential treatment randomization assumption. Yang and Lok (2017) relaxed this assumption by defining a bias function that quantifies the impact of unmeasured confounding and developed a modified estimator for the class of global SNMMs. Additional work is necessary to assess the impact of possible uncontrolled confounding for the new class of local SNMMs. Alternatively, Guan et al. (2023) introduced a spectral perspective that presents a novel approach to addressing unmeasured spatial confounders, which could be explored in our context. Finally, with the app is continuously collecting more data from the users, one of the interesting future directions would be incorporating the covariates into the treatment effect model and estimate the optimal personalized behavior recommendations.

Acknowledgment

We thank the Editor, an Associate Editor, and two Reviewers for their insightful comments and helpful suggestions on the earlier version of this paper. We would also like to thank Linda Wei for the help with the data.

Supplementary Material

Supplementary materials available online include all technical proofs, additional simulation results, other implementation details, and R functions.

Data Availability

Data subject to third party restrictions.

Funding

This research is supported by NSF DMS 1811245, NCI P01 CA142538, NIA 1R01AG066883, and NIEHS 1R01ES031651.

Conflict of Interests

None declared.

References

- Adibi, S. (2014). *mHealth multidisciplinary verticals*. CRC Press.
- Carroll, R. J., D. Ruppert, and A. H. Welsh (1998). Local estimating equations. *J. Am. Stat. Assoc.* 93, 214–227.
- Chakraborty, B. and E. E. Moodie (2013). *Statistical Methods for Dynamic Treatment Regimes*. Springer, New York.
- Coulombe, J. and S. Yang (2024). Multiply robust estimation of marginal structural models in observational studies subject to covariate-driven observations. *Biometrics*, just accepted.
- Fan, J. and I. Gijbels (1996). *Local Polynomial Modelling and Its Applications*. Chapman & Hall, London: CRC Press.
- Fotheringham, A. S., C. Brunson, and M. Charlton (2003). *Geographically weighted regression: the analysis of spatially varying relationships*. John Wiley & Sons.
- Galindo, C. D., H. Liang, G. Kauermann, and R. J. Carrol (2001). Bootstrap confidence intervals for local likelihood, local estimating equations and varying coefficient models. *Statistica Sinica* 11, 121–134.
- Gelfand, A. E., H.-J. Kim, C. Sirmans, and S. Banerjee (2003). Spatial modeling with spatially varying coefficient processes. *J. Am. Stat. Assoc.* 98, 387–396.
- Guan, Y., G. L. Page, B. J. Reich, M. Ventrucchi, and S. Yang (2023). Spectral adjustment for spatial confounding. *Biometrika* 110, 699–719.
- Holland, P. W. (1986). Statistics and causal inference. *J. Am. Stat. Assoc.* 81, 945–960.
- Johnston, F. H., S. B. Henderson, Y. Chen, J. T. Randerson, M. Marlier, R. S. DeFries, P. Kinney, D. M. Bowman, and M. Brauer (2012). Estimated global mortality attributable to smoke from landscape fires. *Environmental health perspectives* 120(5), 695–701.
- Lee, D., C. Gao, S. Ghosh, and S. Yang (2024). Transporting survival of an hiv clinical trial to the external target populations. *Journal of Biopharmaceutical Statistics*, doi.org/10.1080/10543406.2024.2330216.

- Lee, D., S. Yang, M. Berry, T. Stinchcombe, H. J. Cohen, and X. Wang (2024). genrct: a statistical analysis framework for generalizing rct findings to real-world population. *Journal of Biopharmaceutical Statistics*, doi.org/10.1080/10543406.2024.2333136.
- Lee, D., S. Yang, L. Dong, X. Wang, D. Zeng, and J. Cai (2023). Improving trial generalizability using observational studies. *Biometrics* 79, 1213–1225.
- Lee, D., S. Yang, and X. Wang (2022). Doubly robust estimators for generalizing treatment effects on survival outcomes from randomized controlled trials to a target population. *Journal of Causal Inference* 10, 415–440.
- Li, W., S. Yang, and P. Han (2020). Robust estimation for moment condition models with data missing not at random. *Journal of Statistical Planning and Inference* 207, 246–254.
- Pearl, J. (2009). *Causality* (2 ed.). Cambridge: Cambridge University Press.
- Rappold, A., M. Hano, S. Prince, L. Wei, S. Huang, C. Baghdikian, B. Stearns, X. Gao, S. Hoshiko, W. Cascio, et al. (2019). Smoke sense initiative leverages citizen science to address the growing wildfire-related public health problem. *GeoHealth* 3, 443–457.
- Reich, B. J., S. Yang, Y. Guan, A. B. Giffin, M. J. Miller, and A. Rappold (2021). A review of spatial causal inference methods for environmental and epidemiological applications. *International Statistical Review* 89, 605–634.
- Robins, J. (1986). A new approach to causal inference in mortality studies with a sustained exposure period—application to control of the healthy worker survivor effect. *Mathematical Modelling* 7, 1393–1512.
- Robins, J. and A. Rotnitzky (1997). Analysis of semi-parametric regression models with non-ignorable non-response. *Stat. Med.* 16, 81–102.
- Robins, J. M. (1994). Correcting for non-compliance in randomized trials using structural nested mean models. *Comm. Statist. Theory Methods* 23, 2379–2412.
- Robins, J. M. (2000). Marginal structural models versus structural nested models as tools for causal inference. In *Statistical Models in Epidemiology, the Environment, and Clinical Trials*, pp. 95–133. Springer, New York.
- Robins, J. M., D. Blevins, G. Ritter, and M. Wulfsohn (1992). G-estimation of the effect of prophylaxis therapy for pneumocystis carinii pneumonia on the survival of AIDS patients. *Epidemiology* 3, 319–336.
- Robins, J. M. and M. A. Hernán (2009). Estimation of the causal effects of time-varying exposures. *Longitudinal Data Analysis*, 553–599.
- Rubin, D. B. (1976). Inference and missing data. *Biometrika* 63, 581–592.
- Ruppert, D. (1997). Empirical-bias bandwidths for local polynomial nonparametric regression and density estimation. *J. Am. Stat. Assoc.* 92, 1049–1062.
- Wang, S., J. Shao, and J. K. Kim (2014). An instrumental variable approach for identification and estimation with nonignorable nonresponse. *Statistica Sinica* 24, 1097–1116.
- Yang, S. (2022). Semiparametric estimation of structural nested mean models with irregularly spaced longitudinal observations. *Biometrics* 78, 937–949.

Yang, S. and J. J. Lok (2017). Sensitivity analysis for unmeasured confounding in coarse structural nested mean models. *Statistica Sinica* 28, 1703–1723.

Yang, S., K. Pieper, and F. Cools (2020). Semiparametric estimation of structural failure time model in continuous-time processes. *Biometrika* 107, 123–136.

List of Figures

1	A screen shot of the Smoke Sense App alerting the user of local fires and air quality.	4
2	Maximum daily HMS smoke density level in each three-digit zip code over the study period. The smoke density has four levels: None, Light, Medium, and Heavy (corresponding to 0, 5, 16, and 27 $\mu\text{g}/\text{m}^3$, respectively). The vertical line is at longitude -115.	5
3	The number of users in each three-digit zip code over the study period. The vertical line is at longitude -115.	6
4	Global treatment effect curve by time lag. The lag ($k - m$) is the time between treatment (at the m th month) and outcome (at the k th month). The solid line is the treatment effect $\gamma_{m,k}(\hat{\psi}^*)$ evaluated at the estimated values $\hat{\psi}^* = (\hat{\delta}, \hat{\mu}, \hat{\sigma}^2) = (-0.3, 7.0, 3.0)$. The dashed lines are the 95% confidence bands constructed from 200 bootstrapped samples.	17
5	Estimated treatment effect $\hat{\delta}$ for the 28 locations in the Western US. The shapes of symbols denote whether $\hat{\delta}$ is insignificant, significantly negative (SN) or significantly positive (SN). The background color is the maximum daily HMS smoke density in each three-digit zip code. The units of effect is the number of symptoms.	18
6	Variable importance plot of the random forest regression model in terms of the mean decrease in residual sum of squares.	19
7	Location (left) and 95% confidence intervals of treatment effects (right) for the selected cities and national parks. The vertical black dash line is the global treatment effect estimate.	19